

# A Base-Resistant Metalloporphyrin Metal–Organic Framework for C–H Bond Halogenation

Xiu-Liang Lv,<sup>†,‡</sup> Kecheng Wang,<sup>‡,§</sup> Bin Wang,<sup>†</sup> Jie Su,<sup>§</sup> Xiaodong Zou,<sup>§</sup> Yabo Xie,<sup>†</sup> Jian-Rong Li,<sup>\*,†</sup> and Hong-Cai Zhou<sup>\*,‡</sup>

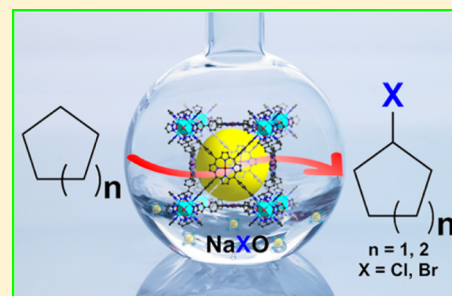
<sup>†</sup>Beijing Key Laboratory for Green Catalysis and Separation and Department of Chemistry and Chemical Engineering, College of Environmental and Energy Engineering, Beijing University of Technology, Beijing 100124, PR China

<sup>‡</sup>Department of Chemistry, Texas A&M University, College Station, Texas 77842-3012, United States

<sup>§</sup>Berzelii Centre EXSELENT on Porous Materials and Inorganic and Structural Chemistry, Department of Materials and Environmental Chemistry, Stockholm University, Stockholm SE-10691, Sweden

## Supporting Information

**ABSTRACT:** A base-resistant porphyrin metal–organic framework (MOF), namely PCN-602 has been constructed with 12-connected  $[\text{Ni}_8(\text{OH})_4(\text{H}_2\text{O})_2\text{Pz}_{12}]$  (Pz = pyrazolate) cluster and a newly designed pyrazolate-based porphyrin ligand, 5,10,15,20-tetrakis(4-(pyrazolate-4-yl)-phenyl)porphyrin under the guidance of the reticular synthesis strategy. Besides its robustness in hydroxide solution, PCN-602 also shows excellent stability in aqueous solutions of  $\text{F}^-$ ,  $\text{CO}_3^{2-}$ , and  $\text{PO}_4^{3-}$  ions. Interestingly, the  $\text{Mn}^{3+}$ -porphyrinic PCN-602, as a recyclable MOF catalyst, presents high catalytic activity for the C–H bond halogenation reaction in a basic system, significantly outperforming its homogeneous counterpart. For the first time, a porphyrinic MOF was thus used as an efficient catalyst in a basic solution with coordinating anions, to the best of our knowledge.



## INTRODUCTION

Metal–organic frameworks (MOFs), emerging as a new class of porous materials, developed at an extraordinary pace over the past two decades.<sup>1</sup> They extended the field of porous materials and showed excellent potential in numerous applications, including catalysis, gas storage/separation, sensing, luminescence, drug delivery and so forth.<sup>2</sup> Porphyrinic MOFs, as a special group of MOFs, have been tremendously studied because of not only the importance of porphyrinic species in many applications, but also the inherent advantages of MOFs as the platforms to immobilize porphyrin groups.<sup>3,4</sup> The rigid structures, large surface area and high porosity of MOFs can not only improve the catalytic activity of porphyrin by preventing the aggregation of reaction centers, but also increase the density of approachable active sites without suffering from low solubility of porphyrin derivatives.<sup>4</sup>

However, to exploit these desirable features of porphyrinic MOFs, the materials should be stable under the harsh chemical conditions involved in real applications. So far, the explorations of the robustness of MOFs are mainly focused on their chemical stability in water and acid aqueous solutions, but the chemical resistance of MOFs toward other species has not been extensively studied.<sup>5</sup> Many coordinating anions (Lewis bases), such as  $\text{F}^-$ ,  $\text{CO}_3^{2-}$ , and  $\text{PO}_4^{3-}$ , are also frequently involved in kinds of reactions.<sup>6</sup> They are usually essential reactants or work as compositions of buffer solutions to control the pH in some reactions catalyzed by porphyrin derivatives. Therefore, strong

resistance of porphyrinic MOFs toward these coordinating anions is also of significance to extend their application scopes.

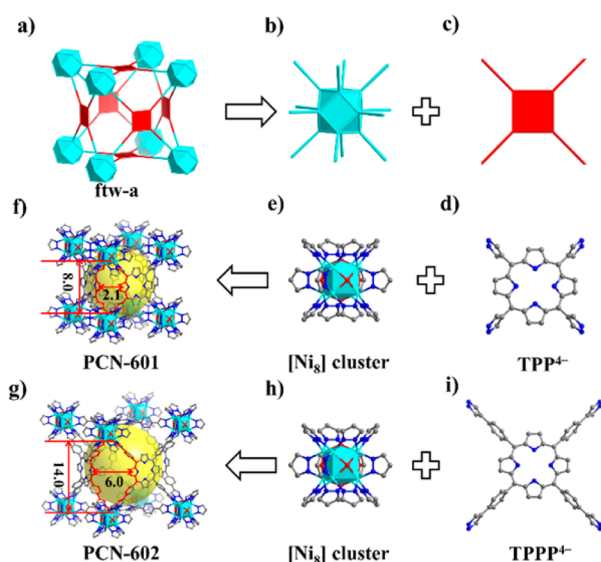
It was found that many reported stable porphyrinic MOFs are constructed with carboxylate-based ligands and  $\text{Zr}^{4+}$ ,  $\text{Fe}^{3+}$ , or  $\text{Al}^{3+}$ -based inorganic clusters.<sup>5d–f</sup> In the hard–soft–acid–base (HSAB) theory, the carboxylate groups and these high valent metal ions are categorized as hard Lewis bases and acids, and can form strong coordination bonds with each other, which endows the frameworks with strong robustness. On the other hand, many coordinating anions, like  $\text{F}^-$ ,  $\text{CO}_3^{2-}$ , and  $\text{PO}_4^{3-}$ , have either small diameters or high charges. They are also classified as Lewis base with great hardness. It leads to their strong affinity toward the high valent metal ions, which is confirmed by the high binding constants of these anions and  $\text{Zr}^{4+}$ ,  $\text{Fe}^{3+}$ , and  $\text{Al}^{3+}$ .<sup>7</sup> As we proposed in our previous work, the decomposition of MOFs in solutions can be considered as the competition between coordination groups of ligands and other molecules (or anions) for metal ions of the inorganic clusters inside the frameworks.<sup>5g</sup> For the MOFs constructed by high valent metal ions, when other hard Lewis bases existing as competing species with high concentration in solution, the carboxylate groups of ligands coordinated to metal ions will be easily replaced, which leads to the MOF decomposition. To overcome the vulnerability of these materials in the solutions of

Received: September 8, 2016

Published: December 11, 2016

coordinating anions with great hardness, one method is to construct MOFs with metal ions and ligands that have higher softness. With this strategy, the strong coordination interaction between the metal ions and ligands can be kept, while the affinity between coordinating anions in the solutions and metal ions inside the frameworks is weakened. This will endow MOFs with strong resistance to the attack of coordinating anions with great hardness.

Recently, our group reported a MOF, namely PCN-601, that fulfill all the requirements mentioned above. It is constructed by  $\text{Ni}^{2+}$  (as  $[\text{Ni}_8]$  cluster  $[\text{Ni}_8(\text{OH})_4(\text{H}_2\text{O})_2\text{Pz}_{12}]$ ,<sup>8</sup> Pz = pyrazolate) and 5,10,15,20-tetra(pyrazolate-4-yl)porphyrin- $(\text{TPP}^{4-})$  ligand, which are soft Lewis acid and base, respectively (Figure 1d–f).<sup>5g</sup> However, the window size of the cages in



**Figure 1.** Reticular design and construction of PCN-602: (a) *ftw-a* topological net; (b) 12-connected node with  $O_h$  symmetry; (c) 4-connected node with  $D_{4h}$  symmetry; (d)  $\text{TPP}^{4-}$  ligand; (e and h)  $[\text{Ni}_8]$  cluster; (f) structure of PCN-601 (Ni atoms in the porphyrin center are omitted for clarity); (g) proposed structure of PCN-602; and (i)  $\text{TPPP}^{4-}$  ligand.

PCN-601 is too small ( $\sim 2.1 \times 8.0$  Å after deducting van der Waals Radii). When PCN-601 is applied as a catalyst, the small window size would slow down the diffusion of reactants or even limit the approachability of active sites for substrates. A direct method to augment the window size and improve catalytic performance is to construct an isorecticular MOF with the rationally designed elongated ligand under the guidance of the reticular synthesis strategy (Figure 1).<sup>9</sup>

We finally chose 5,10,15,20-tetrakis(4-(1*H*-pyrazol-4-yl)-phenyl)porphyrin ( $\text{H}_4\text{TPPP}$ ) as the ligand acid, based on two major considerations. First, in  $\text{TPPP}^{4-}$ , each phenyl ring is vertical to porphyrin center owing to the steric hindrance of pyrazolate groups, while the pyrazolate groups prefer to be parallel to the connected phenyl rings to enlarge the conjugated system and lower the energy of molecule. As a result, in its desired conformation,  $\text{TPPP}^{4-}$  is a 4-connected  $D_{4h}$  symmetric ligand with 4 pyrazolate groups vertical to the porphyrin center, which is symmetrically and geometrically equivalent to  $\text{TPP}^{4-}$ . Therefore, the construction of an isorecticular framework of PCN-601 with  $[\text{Ni}_8]$  and  $\text{TPPP}^{4-}$  would be possible. Second, given the fact that the pore size and stability of a MOF are usually inversely correlated, extensive elongation of the ligand

could undermine the robustness of resulting framework. Comparing with  $\text{TPP}^{4-}$ , only one phenyl ring is inserted between the porphyrin center and pyrazolate groups in  $\text{TPPP}^{4-}$ , which makes it one of the shortest elongated versions of  $\text{TPP}^{4-}$ . Furthermore, the structural simulation suggests that the window size in the resulting MOF is about  $6.0 \times 14.0$  Å, which is large enough for some substrates to diffuse inside its framework. The MOF constructed by  $\text{TPPP}^{4-}$  may thus strike the balance between cavity and robustness of the material.

Here, we report this rationally designed pyrazolate-based MOF,  $[\text{Ni}_8(\text{OH})_4(\text{H}_2\text{O})_2(\text{TPPP-Ni})_3]$ , namely PCN-602(Ni). The experimental results of its stability tests show this material has excellent robustness in aqueous solutions with  $\text{OH}^-$ ,  $\text{F}^-$ ,  $\text{CO}_3^{2-}$ , and  $\text{PO}_4^{3-}$  ions. An isostructural MOF with  $\text{Mn}^{3+}$ -porphyrin ligand ( $\text{TPPP-MnCl}$ )<sup>4+</sup> was then prepared, assigned as PCN-602(Mn). Catalytic activity of PCN-602(Mn) has been demonstrated by its extraordinary performance as a regenerable heterogeneous catalyst in the halogenation of hydrocarbons in basic condition. Compared to previous method with homogeneous Mn-porphyrin catalysts,<sup>10</sup> much higher yields were achieved under more environment-friendly condition with PCN-602(Mn).

## EXPERIMENTAL SECTION

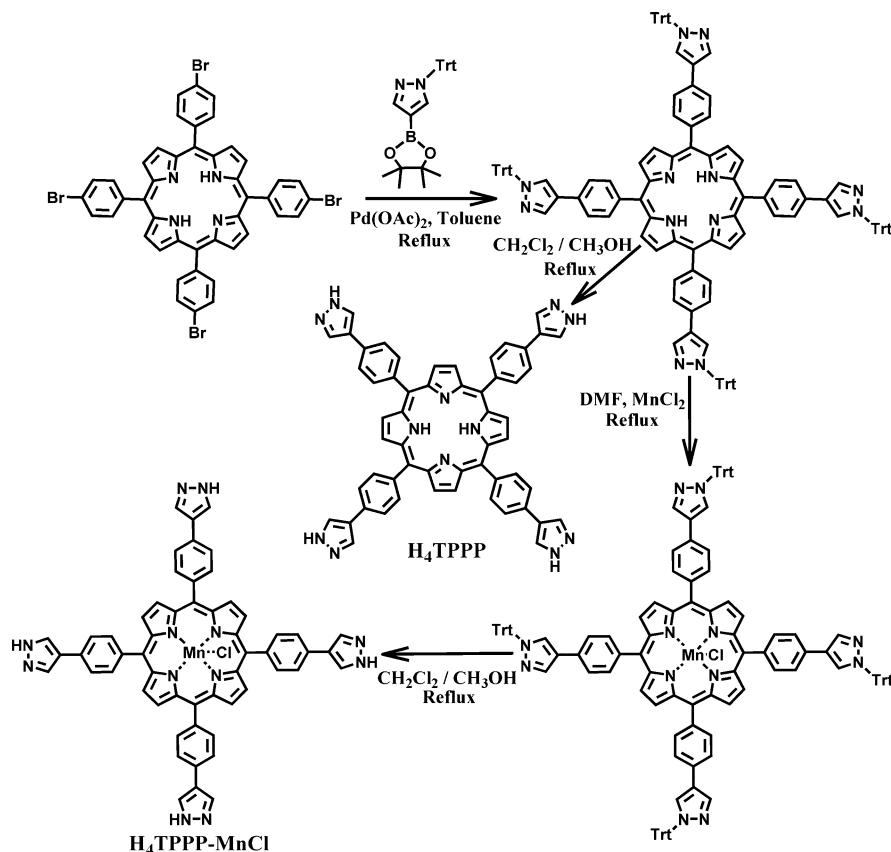
**General Information.** The commercial chemicals are used as purchased unless mentioned otherwise. Detailed chemical sources are listed in the Supporting Information section 1.

**Instrumentation.** Synchrotron powder X-ray diffraction (PXRD) was carried out with Bruker D8-Discover diffractometer equipped with a Mo sealed tube ( $\lambda = 0.45336$  Å) on the beamline 17-BM at the Advanced Photon Source, Argonne National Laboratory. Other PXRD experiments were carried out on a BRUKER D8-Focus Bragg-Brentano X-ray powder Diffractometer equipped with a Cu sealed tube ( $\lambda = 1.54178$  Å) at 40 kV and 40 mA. NMR data were collected on a Mercury 400 NMR spectrometer. FT-IR spectra were recorded on an IR Affinity-1 instrument. Thermogravimetric analysis (TGA) data were obtained on a TGA-50 (SHIMADZU) thermogravimetric analyzer with a heating rate of  $10$  °C  $\text{min}^{-1}$  under air atmosphere.  $\text{N}_2$  adsorption-desorption isotherms were measured using a Micromeritics ASAP 2420 system at 77 K. The UV-vis absorption spectra were recorded on a Shimadzu UV-2450 spectrophotometer. The morphologies of the MOF sample were observed by using a SU8020 Scanning Electron Microscope (SEM) (Hitachi, Japan). Elemental analysis (EA) was performed by vario EL cube Elementar. Inductively Coupled Plasma-Optical Emission spectroscopic (ICP-OES) data were collected on a Thermo iCAP-6300 Spectrometer. The conversions of the reactants and the yields of products were measured by Bruker Scion TQ GC-MS equipped with BR-5MS capillary column.

**Synthesis of  $\text{H}_4\text{TPPP}$  and  $\text{H}_4\text{TPPP-MnCl}$ .** The synthesis procedure is shown in Scheme 1 and details are in the Supporting Information section 2.

**Synthesis of PCN-602(Ni).**  $\text{Ni}(\text{AcO})_2 \cdot 4\text{H}_2\text{O}$  (8 mg, 32.3 mmol),  $\text{H}_4\text{TPPP}$  (10 mg, 17.4 mmol), and deionized (DI) water (1.2 mL) in 2 mL of *N,N*-dimethylformamide (DMF) were mixed and ultrasonically dissolved in a 5 mL high-pressure vessel. The resulting mixture was sealed and heated at 120 °C for 24 h. After the vial cooled down to room temperature, reddish crystalline powder of PCN-602(Ni) was collected by filtration (8 mg). FT-IR spectrum of as-synthesized PCN-602(Ni) is shown in Figure S1 of the Supporting Information. The SEM image indicates that the crystal size of obtained powder is around 100 nm (Figure S3 in the Supporting Information). TGA curve reveals that the thermal stability of PCN-602(Ni) can be held up to 280 °C, from which it begins to decompose (Figure S4 in the Supporting Information).

**Synthesis of PCN-602(Mn).**  $\text{Ni}(\text{AcO})_2 \cdot 4\text{H}_2\text{O}$  (6 mg, 24.2 mmol),  $\text{H}_4\text{TPPP-MnCl}$  (10 mg, 15.0 mmol), DI water (2.5 mL), and DMF (1.5 mL) were mixed in a 5 mL high-pressure vessel. The mixture was

Scheme 1. Synthesis of H<sub>4</sub>TPPP and H<sub>4</sub>TPPP-MnCl

sealed and heated at 120 °C for 24 h. After the vial cooled down to room temperature, dark green crystalline powder of PCN-602(Mn) was collected by filtration (8 mg). FT-IR spectrum of as-synthesized PCN-602(Mn) is shown in Figure S2 of the [Supporting Information](#). TGA curve reveals that the thermal stability of PCN-602(Mn) can be held up to 280 °C, from which it begins to decompose (Figure S5 in the [Supporting Information](#)).

**Rietveld Refinement and Crystallographic Data of PCN-602(Ni).** The structure model of PCN-602(Ni) was refined by Rietveld refinement using Topas Academic version 4.1. Background was fitted with a 15th order Chebyshev polynomial. The refinement was conducted using a Pearson VII type peak profile function, followed by refinement of unit cells and zero-shift. Soft distance restraints were placed on the bonds between the nickel and oxygen atoms (2.20 Å), and the nickel and nitrogen atoms (2.10 Å). The rigid bodies were applied on ligands. The ligand was not fully occupied. The occupancy was refined to be 0.76. The additional oxygen atom (O2) with the occupancy of 0.24 was located near nickel atom (Ni1) with the Ni–O bond distance of 2.21 Å. The guest species in the cages of the structure could not be located owing to their partial occupancies and low symmetry. Instead, three oxygen atoms were added at random positions inside the cages to compensate for the contributions of the guest species, and refined subsequently. Crystallographic data and structural refinement are provided in [Table 1](#).

**Gas Adsorption of PCN-602(Ni) and -602(Mn).** The reddish/dark green powders of PCN-602(Ni)/602(Mn) obtained through the solvothermal reaction were washed with DMF and DI water for several times. Then the samples were washed with acetone for 3 times. After being soaked in acetone for 12 h, the samples were activated at 100 °C under vacuum for 10 h. Then, their N<sub>2</sub> uptakes were measured at 77 K, respectively.

**PXRD Measurements for Stability Test of PCN-602(Ni).** After being washed with DMF and DI water, as-obtained PCN-602(Ni) samples (10 mg for each batch) were immersed in about 3.5 mL aqueous solutions of 0.1 mM HCl (pH = 4), 1 M NaOH (pH = 14), 1

**Table 1. Crystallographic Data and the Rietveld Refinement Result of PCN-602(Ni)**

compound	PCN-602(Ni)
chemical formula	C <sub>127.92</sub> H <sub>73.12</sub> N <sub>27.44</sub> Ni <sub>10.24</sub> O <sub>21.98</sub>
Formula weight	2948.80
Crystal system	cubic
Space group	<i>Pm</i> $\bar{3}$ <i>m</i>
<i>a</i> /Å	21.559(2)
<i>Z</i>	1
Temperature/K	298(2)
Wavelength/Å	0.45336
2θ range/°	0.8–21.39
Number of reflections	686
Number of structural variables	49
<i>R</i> <sub>p</sub>	0.03849
<i>R</i> <sub>wp</sub>	0.04896
<i>R</i> <sub>exp</sub>	0.00938
GOF	5.219

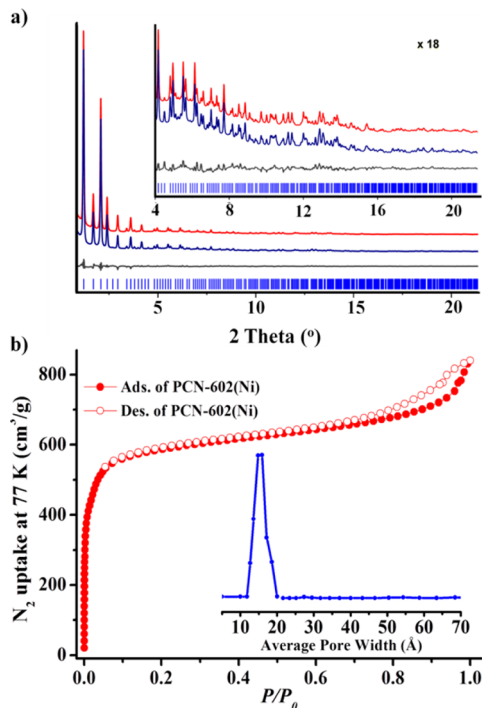
M KF, 1 M Na<sub>2</sub>CO<sub>3</sub>, and 1 M K<sub>3</sub>PO<sub>4</sub> at room temperature for 24 h, respectively. The treated samples were collected and washed successively with DI water (3 times) and acetone (3 times). The obtained powders were dried in oven at 100 °C before PXRD measurements.

**N<sub>2</sub> Uptakes for Stability Test of PCN-602(Ni).** Five batches of samples (about 100 mg for each) were immersed in 35 mL of 0.1 mM HCl (pH = 4), 1 M NaOH (pH = 14), 1 M KF, 1 M Na<sub>2</sub>CO<sub>3</sub>, and 1 M K<sub>3</sub>PO<sub>4</sub> aqueous solutions at room temperature (RT) for 24 h, respectively. After being collected and washed with DI water (3 times) and acetone (3 times), the samples were activated under vacuum at 100 °C for 10 h on ASAP 2420 system. These activated samples were then measured for N<sub>2</sub> sorption at 77 K.

**Catalysis.** The C–H bond halogenations reactions were conducted under two conditions. **Condition 1:** Catalyst (13 mmol), NaClO (2 mL, 0.33 M in water), tetrabutylammonium chloride (TBACl, 8 mg, as the phase transfer catalyst (PTC)), substrate (2 mmol), and dichloromethane (2 mL) were mixed and stirred under nitrogen at RT for 5 h. **Condition 2:** Catalyst (13 mmol), NaClO (2 mL, 0.33 M in water), substrate (2 mmol), and acetone (2 mL) were mixed and stirred under nitrogen at RT for 2 h. After the completion of the reaction, the heterogeneous catalyst was collected by filtration. The homogeneous catalyst, inorganic salt and PTC in the filtrate were removed by a short silica gel column eluted by  $\text{CH}_2\text{Cl}_2$ . Then, the identities and the yields of the products were determined by GC-MS. (detailed information is in section 13 of Supporting Information)

## RESULTS AND DISCUSSION

The structural model of PCN-602 with a space group of  $Pm\bar{3}m$  was derived from PCN-601 and constructed by Material Studio 6.0 (Figure 1g). The unit cell parameter of  $a = 21.559 \text{ \AA}$  was obtained through indexing experimental high-resolution PXRD data of PCN-602(Ni). The predicted structure was further refined by Rietveld refinement against the synchrotron PXRD data with Topas Academic version 4.1 (Figure 2a). The

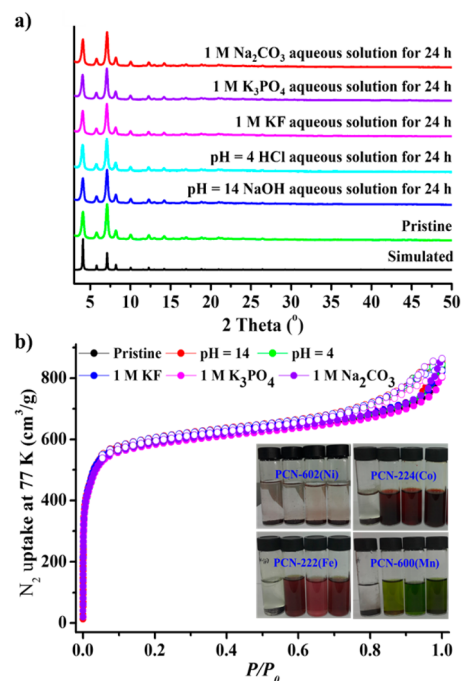


**Figure 2.** (a) Rietveld refinement of powder X-ray diffraction data for PCN-602(Ni) (the curves from top to bottom are simulated (red), observed (blue), and difference profiles (gray), respectively); the bars below curves indicate peak positions; and (b)  $\text{N}_2$  adsorption/desorption isotherms of activated PCN-602(Ni) at 77 K (inset shows DFT pore size distribution evaluated from the  $\text{N}_2$  adsorption data at 77 K).

resulting structure of PCN-602(Ni) has a larger window size of  $6.3 \times 14.2 \text{ \AA}$  than that of PCN-601 ( $2.1 \times 8.0 \text{ \AA}$ ). The  $\text{N}_2$  isotherm of activated PCN-602(Ni) at 77 K reveals a Brunauer–Emmett–Teller (BET) surface area of  $2219 \text{ m}^2 \text{ g}^{-1}$  and total pore volume of  $1.36 \text{ cm}^3 \text{ g}^{-1}$  (Figure 2b), being significantly larger than those of PCN-601.<sup>5g</sup>

Chemical stability of PCN-602(Ni) was first tested by treating its samples with the aqueous solutions of HCl and NaOH with pH = 4 and 14 for 24 h at RT, respectively. The

PXRD patterns of the treated samples remained intact, indicating there was no phase transition or entire framework collapse of PCN-602(Ni) after the treatments (Figure 3a).  $\text{N}_2$



**Figure 3.** (a) PXRD patterns simulated from the PCN-602 structural model, of pristine PCN-602(Ni) sample, and of those treated in different aqueous solutions and (b)  $\text{N}_2$  adsorption/desorption isotherms of pristine PCN-602(Ni) sample and of those treated in different aqueous solutions (inset: photographs of PCN-602(Ni), -224(Co), -222(Fe), and -600(Mn) soaked in different solutions for 24 h: DI water, 1 M KF, 1 M  $\text{Na}_2\text{CO}_3$ , and 1 M  $\text{K}_3\text{PO}_4$  aqueous solutions, from left to right).

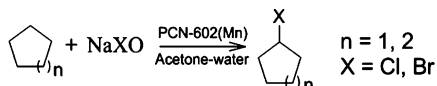
isotherms at 77 K of these treated samples further confirmed the robustness of PCN-602(Ni) in the acid and base solutions (Figure 3b). Moreover, we also explored the stability of PCN-602(Ni) in 1 M KF, 1 M  $\text{Na}_2\text{CO}_3$  and 1 M  $\text{K}_3\text{PO}_4$  aqueous solutions, respectively. After soaking PCN-602(Ni) in these solutions for 24 h at RT, PXRD patterns and  $\text{N}_2$  isotherms of treated samples remained unchanged, demonstrating its excellent stability in these solutions. For comparison, when PCN-224(Co), -222(Fe) and -600(Mn) were treated under the same conditions, the deep color of the solutions and the dissolution of the solid phases clearly indicated the severe decomposition of these MOFs (Figure 3b, inset). Considering  $\text{F}^-$ ,  $\text{CO}_3^{2-}$  and  $\text{PO}_4^{3-}$  are all the conjugate bases of weak acids, the hydrolysis of these anions in aqueous solution will produce hydroxide anions, which are also destructive to the MOFs. To assess the effect of hydroxide anions in the decomposition of PCN-224(Co), -222(Fe) and -600(Mn), the pH values of 1 M KF, 1 M  $\text{Na}_2\text{CO}_3$  and 1 M  $\text{K}_3\text{PO}_4$  solutions were measured (Table S1). For instance, the pH value of 1 M KF solution was 7.79, while PCN-224(Co) -222(Fe) and -600(Mn) were claimed to be stable in NaOH aqueous solution with the pH value of 9.<sup>4b,5e</sup> The complete dissolution of these three MOFs in 1 M KF aqueous solution should be attributed to attack of  $\text{F}^-$  anions. As revealed by the results above, when we evaluate the robustness of porphyrinic MOFs for the real applications, not only their stability in hydroxide solutions but also their resistance toward the attack of other coordinating anions

should be carefully considered. However, the later requirement has been neglected for a long time, and can hardly be met by the previously reported on porphyrinic MOFs.

As we known, alkyl halides are widely applied in chemical industry and afford important components of a variety of biologically and pharmacologically active molecules.<sup>11</sup> Accordingly, the development of new synthesis approaches for alkyl halides is quite interesting but challenging, especially for the direct halogenation of inert C–H bonds. In 2010, Groves and his co-workers reported a method to directly halogenate alkylates with manganese porphyrin as the catalyst and hypohalite as the halogen source.<sup>10</sup> However, this method still suffered from the moderate yields and the usage of homogeneous catalyst, which makes the recovery of the catalyst difficult. As we mentioned above, immobilizing porphyrin into MOFs could be an efficient method to improve the activity and recyclability of catalysts. Unfortunately, most of the reported porphyrinic MOFs cannot resist the attack of hydroxide and other coordinating anions in this reaction condition. As expected, the intergeneration of large porosity, high concentration of potentially catalytically active sites, and extreme chemical stability in solutions of hydroxide and other coordinating anions makes PCN-602 a great candidate for the heterogeneous catalyst of this reaction.

The PCN-602 with Mn<sup>3+</sup>-porphyrin centers (assigned as PCN-602(Mn)) was synthesized. Its chemical stability in acidic, basic and coordinating anion containing aqueous solutions was also tested (section 9 in the Supporting Information). The results demonstrated its stability is as high as that of PCN-602(Ni). Then, we applied PCN-602(Mn) as the catalyst in the halogenation reaction (Scheme 2). By following the reaction

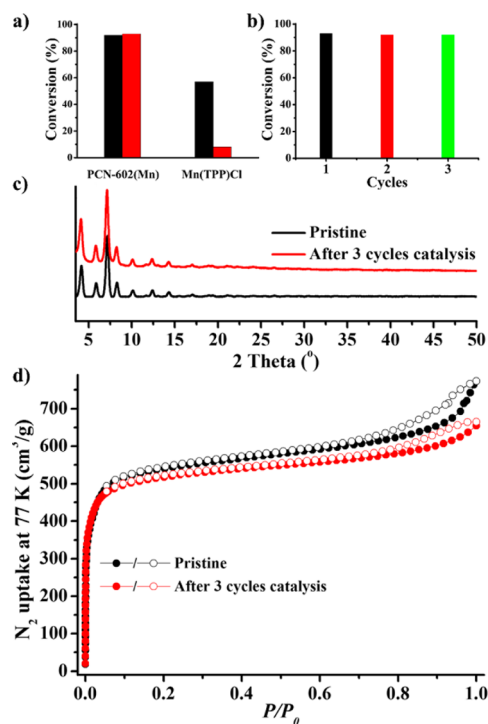
**Scheme 2. C–H Bond Halogenation Catalyzed by PCN-602(Mn)**



condition described in Grove's paper,<sup>10</sup> PCN-602(Mn) (5 mg), NaClO (2 mL, 0.33 M in water), TBACl (8 mg), cyclohexane (0.22 mL, 2 mmol), and dichloromethane (2 mL) were mixed and stirred under nitrogen at RT for 5 h. A 92% yield of chlorocyclohexane was achieved. It is much higher than that reported in Grove's paper (57%) when homogeneous catalyst, Mn(TPP)Cl (herein, H<sub>2</sub>TPP = *meso*-tetraphenylporphyrin) was applied.<sup>10</sup> The higher catalytic activity of PCN-602(Mn) could be explained by its rigid framework structure. When porphyrin catalysts are dissolved, the formation of catalytically inactive dimers is almost inevitable. As comparison, the porphyrinic ligands are separated and anchored at the fixed positions in PCN-602(Mn), which makes every porphyrin center highly active.

Moreover, with PCN-602(Mn) as the catalyst, further optimization could be achieved for this reaction. In the above-mentioned condition, two toxic species, dichloromethane and PTC, are applied to dissolve catalyst better and/or facilitate the immigration of ClO<sup>−</sup> from aqueous phase to organic phase to react with catalyst. However, the rigid structure and high porosity of PCN-602(Mn) can provide high density of active sites that are approachable to the substrates, which makes the solubility of the catalyst and the phase transfer rate of ClO<sup>−</sup> not the limiting factors any more. This encouraged us to develop a

reaction procedure with more environment-friendly solvent and no PTC (Table S3 in the Supporting Information). After systematic exploration, acetone was finally chosen as the best organic solvent. The yield of the chlorocyclohexane reached 93% at RT in an even shorter time (2 h) under this condition. As a comparison, when Mn(TPP)Cl was used as the catalyst under this condition, the product yield was only 8% (Figure 4a and Table 2).

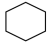
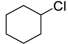
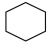
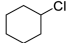
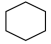
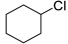

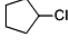
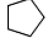
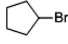
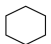
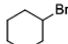


**Figure 4.** (a) Catalytic efficiencies of PCN-602(Mn) and Mn(TPP)Cl in the cyclohexane chlorination in the presence of PTC and CH<sub>2</sub>Cl<sub>2</sub> (black) and under the optimal conditions in this work without PTC (red); (b) Catalytic efficiencies of PCN-602(Mn) in three consecutive cyclic runs; and (c) PXRD patterns and (d) N<sub>2</sub> adsorption/desorption isotherms (at 77 K) of pristine PCN-602(Mn) and that after 3 catalytic cycles, respectively.

In addition, to evaluate the effect of pore-window size of the MOFs on the catalytic performance, PCN-601(Mn) was also prepared and applied as catalyst in the cyclohexane chlorination under the same optimized condition. After an even longer reaction time of 10 h, the yield was only up to 15%. Clearly, the small window sizes of the cages in PCN-601(Mn) blocks the accesses of substrates to the active sites inside the framework, and thereby reduces its catalytic activity.

It should also be pointed out that the recyclability is another significant advantage of solid heterogeneous catalysts. To assess the performance of PCN-602(Mn) as a regenerable catalyst, the cycling experiment was conducted. After one run of reaction in acetone–water, the catalyst was collected through centrifugation and reused in the next run of reaction under the same condition. It was found that after three consecutive cycles, PCN-602(Mn) was still highly active with the reaction yield maintaining up to 92% (Figure 4b). Moreover, the unchanged PXRD pattern and the N<sub>2</sub> adsorption isotherm of PCN-602(Mn) in Figure 4c and 4d further confirmed its structural intactness after the cycling experiment.

**Table 2. Catalytic Performance of PCN-602(Mn) and Other Selected Catalysts in the C–H Bond Chlorination/Bromination of Cyclohexane/Cyclopentane<sup>a</sup>**

Entry	Substrate	Catalyst	Product	Yield(%)
1		PCN-602(Mn)		93 <sup>a</sup>
2		Mn(TPP)Cl		8 <sup>a</sup>
3		PCN-601(Mn)		15 <sup>b</sup>
4		PCN-602(Mn)		95 <sup>a</sup>
5		PCN-602(Mn)		89 <sup>c</sup>
6		PCN-602(Mn)		85 <sup>c</sup>

<sup>a</sup>Standard conditions: substrate/NaClO/catalyst = 2:0.66:0.013 mmol; in acetone–water (2:2 mL); and the suspension was stirred at RT for 2 h. <sup>b</sup>The reaction time is extended to 10 h. <sup>c</sup>NaBrO was used instead of NaClO.

The application scope of this MOF catalyst was also extended to the chlorination of cyclohexane and the bromination of alkylane substrates. The high yields were achieved under similar reaction conditions, with the chlorination of cyclohexane up to 93% and the bromination of cyclohexane and cyclopentane up to 85 and 89%, respectively.

Overall, the above results demonstrate that high-yield aliphatic halogenations can be achieved with PCN-602(Mn) as a regenerable heterogeneous catalyst under a more environment-friendly condition. This MOF catalyst significantly outperformed its homogeneous counterparts. To the best of our knowledge, this is the first example for the application of porphyrinic MOFs as highly efficient catalyst in a harsh basic reaction condition.

In conclusion, guided by the reticular synthesis strategy, a base-resistant pyrazolate-based porphyrinic MOF with high porosity and large window size, namely PCN-602, was constructed. It shows extraordinary robustness in basic solutions of several coordinating anions that are widely used in catalytic reactions. PCN-602(Mn), with Mn<sup>3+</sup>-porphyrin centers was confirmed to be a highly effective heterogeneous catalyst for the C–H halogenation of inert hydrocarbons under a basic condition. The base resistance of PCN-602 greatly broadens the application scope of MOFs as catalysts.

## ■ ASSOCIATED CONTENT

### Supporting Information

The Supporting Information is available free of charge on the ACS Publications website at DOI: 10.1021/jacs.6b09463.

Full details for the synthesis and characterizations of the ligands and MOFs, SEM, FT-IR, N<sub>2</sub> isotherms, BET calculation, pore size distribution, thermal and chemical stability tests, and catalysis activity test (PDF)

Crystallographic data of the refined structure (CIF)

## ■ AUTHOR INFORMATION

### Corresponding Authors

\*jrli@bjut.edu.cn

\*zhou@chem.tamu.edu

## ORCID

Jian-Rong Li: 0000-0002-8101-8493

Hong-Cai Zhou: 0000-0002-9029-3788

## Author Contributions

#X.-L.L. and K.W. contributed equally to this work.

## Notes

The authors declare no competing financial interest.

## ■ ACKNOWLEDGMENTS

This work was financially supported by the Natural Science Foundation of China (21576006); the Center for Gas Separations Relevant to Clean Energy Technologies, an Energy Frontier Research Center funded by the U.S. Department of Energy, Office of Science, Basic Energy Sciences (DE-SC00010150); and the Swedish Research Council (VR) for the MATsynCELL project, and the Knut & Alice Wallenberg Foundation for the 3DEM-NATUR project.

## ■ REFERENCES

- (1) (a) Zhou, H.-C.; Long, J. R.; Yaghi, O. M. *Chem. Rev.* **2012**, *112*, 673. (b) Zhou, H.-C.; Kitagawa, S. *Chem. Soc. Rev.* **2014**, *43*, 5415.
- (2) (a) Liu, J.; Chen, L.; Cui, H.; Zhang, J.; Zhang, L.; Su, C.-Y. *Chem. Soc. Rev.* **2014**, *43*, 6011. (b) Yoon, M.; Srirambalaji, R.; Kim, K. *Chem. Rev.* **2012**, *112*, 1196. (c) Suh, M. P.; Park, H. J.; Prasad, T. K.; Lim, D.-W. *Chem. Rev.* **2012**, *112*, 782. (d) Sumida, K.; Rogow, D. L.; Mason, J. A.; McDonald, T. M.; Bloch, E. D.; Herm, Z. R.; Bae, T.-H.; Long, J. R. *Chem. Rev.* **2012**, *112*, 724. (e) Li, J.-R.; Sculley, J.; Zhou, H.-C. *Chem. Rev.* **2012**, *112*, 869. (f) Wu, H.; Gong, Q.; Olson, D. H.; Li, J. *Chem. Rev.* **2012**, *112*, 836. (g) Kreno, L. E.; Leong, K.; Farha, O. K.; Allendorf, M.; Van Duyne, R. P.; Hupp, J. T. *Chem. Rev.* **2012**, *112*, 1105. (h) Cui, Y.; Yue, Y.; Qian, G.; Chen, B. *Chem. Rev.* **2012**, *112*, 1126. (i) Horcajada, P.; Gref, R.; Baati, T.; Allan, P. K.; Maurin, G.; Couvreur, P.; Férey, G.; Morris, R. E.; Serre, C. *Chem. Rev.* **2012**, *112*, 1232.
- (3) (a) Gao, W.-Y.; Chrzanowski, M.; Ma, S. *Chem. Soc. Rev.* **2014**, *43*, 5841. (b) Zhao, M.; Ou, S.; Wu, C.-D. *Acc. Chem. Res.* **2014**, *47*, 119. (c) Huh, S.; Kim, S.-J.; Kim, Y. *CrystEngComm* **2016**, *18*, 345.
- (4) (a) Farha, O. M.; Shultz, A. M.; Sarjeant, A. A.; Nguyen, S. T.; Hupp, J. T. *J. Am. Chem. Soc.* **2011**, *133*, 565. (b) Feng, D.; Gu, Z.-Y.; Li, J.-R.; Jiang, H.-L.; Wei, Z.; Zhou, H.-C. *Angew. Chem., Int. Ed.* **2012**, *51*, 10307. (c) Yang, X.-L.; Xie, M.-H.; Zou, C.; He, Y.; Chen, B.; O’Keeffe, M.; Wu, C.-D. *J. Am. Chem. Soc.* **2012**, *134*, 10638. (d) Zhang, Z.; Zhang, L.; Wojtas, L.; Eddaoudi, M.; Zaworotko, M. J. *J. Am. Chem. Soc.* **2012**, *134*, 928. (e) Johnson, J. A.; Zhang, X.; Reeson, T. C.; Chen, Y.-S.; Zhang, J. *J. Am. Chem. Soc.* **2014**, *136*, 15881. (f) Lu, K.; He, C.; Lin, W. *J. Am. Chem. Soc.* **2014**, *136*, 16712. (g) Anderson, J. S.; Gallagher, A. T.; Mason, J. A.; Harris, T. D. *J. Am. Chem. Soc.* **2014**, *136*, 16489. (h) Liu, Y.; Howarth, A. J.; Hupp, J. T.; Farha, O. K. *Angew. Chem., Int. Ed.* **2015**, *54*, 9001. (i) Feng, D.; Chung, W.-C.; Wei, Z.; Gu, Z.-Y.; Jiang, H.-L.; Chen, Y.-P.; Darensbourg, D. J.; Zhou, H.-C. *J. Am. Chem. Soc.* **2013**, *135*, 17105.
- (5) (a) Deria, P.; Gómez-Gualdrón, D. A.; Bury, W.; Schaeff, H. T.; Wang, T. C.; Thallapally, P. K.; Sarjeant, A. A.; Snurr, R. Q.; Hupp, J. T.; Farha, O. K. *J. Am. Chem. Soc.* **2015**, *137*, 13183. (b) Lin, Q.; Bu, X.; Kong, A.; Mao, C.; Zhao, X.; Bu, F.; Feng, P. *J. Am. Chem. Soc.* **2015**, *137*, 2235. (c) Zheng, J.; Wu, M.; Jiang, F.; Su, W.; Hong, M. *Chem. Sci.* **2015**, *6*, 3466. (d) Fateeva, A.; Chater, P. A.; Ireland, C. P.; Tahir, A. A.; Khimyak, Y. Z.; Wiper, P. V.; Darwent, J. R.; Rosseinsky, M. J. *Angew. Chem., Int. Ed.* **2012**, *51*, 7440. (e) Wang, K.; Feng, D.; Liu, T.-F.; Su, J.; Yuan, S.; Chen, Y.-P.; Bosch, M.; Zou, X.; Zhou, H.-C. *J. Am. Chem. Soc.* **2014**, *136*, 13983. (f) Liu, T.-F.; Feng, D.; Chen, Y.-P.; Zou, L.; Bosch, M.; Yuan, S.; Wei, Z.; Fordham, S.; Wang, K.; Zhou, H.-C. *J. Am. Chem. Soc.* **2015**, *137*, 413. (g) Wang, K.; Lv, X.-L.; Feng, D.; Li, J.; Chen, S.; Sun, J.; Song, L.; Xie, Y.; Li, J.-R.; Zhou, H.-C. *J. Am. Chem. Soc.* **2016**, *138*, 914. (h) Mouchaham, G.; Cooper, L.; Guillou, N.; Martineau, C.; Elkaïm, E.; Bourrelly, S.; Llewellyn, P. L.;

- Allain, C.; Clavier, G.; Serre, C.; Devic, T. *Angew. Chem., Int. Ed.* **2015**, *54*, 13297. (i) Cunha, D.; Yahia, M. B.; Hall, S.; Miller, S. R.; Chevreau, H.; Elkaïm, E.; Maurin, G.; Horcajada, P.; Serre, C. *Chem. Mater.* **2013**, *25*, 2767. (j) Horcajada, P.; Serre, C.; Vallet-Regí, M.; Sebban, M.; Taulelle, F.; Férey, G. *Angew. Chem., Int. Ed.* **2006**, *45*, 5974. (k) Serre, C.; Millange, F.; Thouvenot, C.; Noguès, M.; Marsolier, G.; Louër, D.; Férey, G. *J. Am. Chem. Soc.* **2002**, *124*, 13519.
- (6) Denmark, S. E.; Beutner, G. L. *Angew. Chem., Int. Ed.* **2008**, *47*, 1560.
- (7) (a) David, R. L. *CRC Handbook of Chemistry and Physics*, 82nd ed.; CRC Press, 2001. (b) Speiht, J. G. *Lange's Handbook of Chemistry*, 16th ed.; McGraw-Hill Education, 2005.
- (8) (a) Padiál, N. M.; Procopio, E. Q.; Montoro, C.; López, E.; Oltra, J. E.; Colombo, V.; Maspero, A.; Masciocchi, N.; Galli, S.; Senkovska, I.; Kaskel, S.; Barea, E.; Navarro, J. A. R. *Angew. Chem., Int. Ed.* **2013**, *52*, 8290. (b) Masciocchi, N.; Galli, S.; Colombo, V.; Maspero, A.; Palmisano, G.; Seyyedi, B.; Lamberti, C.; Bordiga, S. *J. Am. Chem. Soc.* **2010**, *132*, 7902.
- (9) Yaghi, O. M.; O'Keeffe, M.; Ockwig, N. W.; Chae, H. K.; Eddaoudi, M.; Kim, J. *Nature* **2003**, *423*, 705.
- (10) Liu, W.; Groves, J. T. *J. Am. Chem. Soc.* **2010**, *132*, 12847.
- (11) (a) Fauvarque, J. *Pure Appl. Chem.* **1996**, *68*, 1713. (b) Saikia, I.; Borah, A. J.; Phukan, P. *Chem. Rev.* **2016**, *116*, 6837.